Fatigue Growth of Cohesive Defects in T-Peel Joints

M. D. Gilchrist[a]; R. A. Smith[b]

[a] Department of Mechanical Engineering, Imperial College of Science, Technology & Medicine, London, UK [b] Department of Mechanical & Process Engineering, University of Sheffield, Sheffield, UK

PLEASE SCROLL DOWN FOR ARTICLE

Fatigue Growth of Cohesive Defects in T-Peel Joints*

M. D. GILCHRIST**

Department of Mechanical Engineering, Imperial College of Science, Technology & Medicine, Exhibition Road, London SW7 2BX, UK.

R. A. SMITH

Department of Mechanical & Process Engineering, University of Sheffield, PO Box 600, Mappin Street, Sheffield S1 4DU, UK.

This paper uses 2D and 3D finite element models to predict the stresses within bonded and weld-bonded T-peel joints. Epoxy adhesive is modelled as a homogeneous layer providing a perfect bond between aluminium adherends. Knowledge of the critical tensile stresses enables the likely region of fatigue crack initiation to be predicted. The long term reliability and durability of a joint depend directly on its fatigue strength. This research elucidates the region of cohesive crack initiation, the subsequent direction of crack propagation and the relative duration of the different stages of fatigue crack growth. The various stages of embedded, surface and through-width fatigue growth of cohesive defects within a T-peel joint are compared. This establishes fatigue life from crack initiation to final joint fracture for typical bonded and weld-bonded T-peel joints.

KEY WORDS fatigue; crack propagation; T-peel; finite element method; linear elastic fracture mechanics; weld-bonded joints; aluminium; adhesive bonding.

NOMENCLATURE

a	characteristic dimension of defect
d	spot-weld diameter
da/dN	crack growth rate
m	Paris law material growth rate exponent
w	characteristic dimension of specimen
(x,y,z)	coordinate axes
C	Paris law material growth rate coefficient
E	Young's modulus
E'	$E/(1 - \nu^2)$

G   strain energy release rate
J   J-integral
K   stress intensity factor
N   number of fatigue loading cycles
ν Poisson's ratio
σ stress
ϕ parametric angle defining position on crack front
χ length of adhesive fillet

INTRODUCTION

Industrial spot-welding processes have become widely automated, providing good joints between steel components. Spot-welding of aluminium components has not been as successful for reasons which are only partly understood. The difficulties of spot-welding aluminium are similar to those associated with the spot-welding of zinc-coated and stainless steels and considerable care is required to obtain the uniform weld integrity within such spot-welds which is necessary for satisfactory joint performance. Furthermore, the life of an electrode tip when spot welding aluminium is generally less than when spot welding steels. Approximately 2000 aluminium spot welds can be made before tip dressing is required compared with 10000 for steels.[1] It is partly for these reasons that aluminium T-section joints are made by combining adhesive bonding with the weld-bonding process. A consequence of these processes is that, for a given gauge thickness, the stiffness of bonded and weld-bonded joints is more than that of a welded joint. This increased rigidity is often desirable since it enhances the stability of a joint.

A schematic of a typical T-peel joint between two aluminium plates with an epoxy adhesive is shown in Figure 1. Under this peel loading the stresses are not distributed uniformly throughout the adhesive but rather are concentrated within a fine region close to the edge of the joint. Static or fatigue failure is therefore likely to occur unless the bond size is large or the load small. It is not immediately evident whether a spot-weld provides a stronger bond than an adhesive since this depends on the precise location and size of the weld and the extent and material of the adhesive layer. It certainly depends on the uniformity and integrity with which either type of joint is made. Likewise it is unclear what if indeed any benefit to joint strength is provided by a spot-weld when used in conjunction with an adhesive bond (*i.e.,* weld-bonding *vs.* bonding).

Within bonded joints there are two distinct ways in which a defect can propagate: adhesive (interfacial) crack growth occurs along the interface between adhesive and adherend whilst cohesive growth is contained wholly within the adhesive layer. Under certain conditions one or other of these modes of propagation will dominate. Within T-peel joints cohesive crack growth tends to dominate although neither the precise region of crack initiation nor direction of propagation are completely understood. This particular work elucidates these factors by determining the distribution of stresses within the adhesive layer prior to the formation of a defect and also in the presence of a defect.
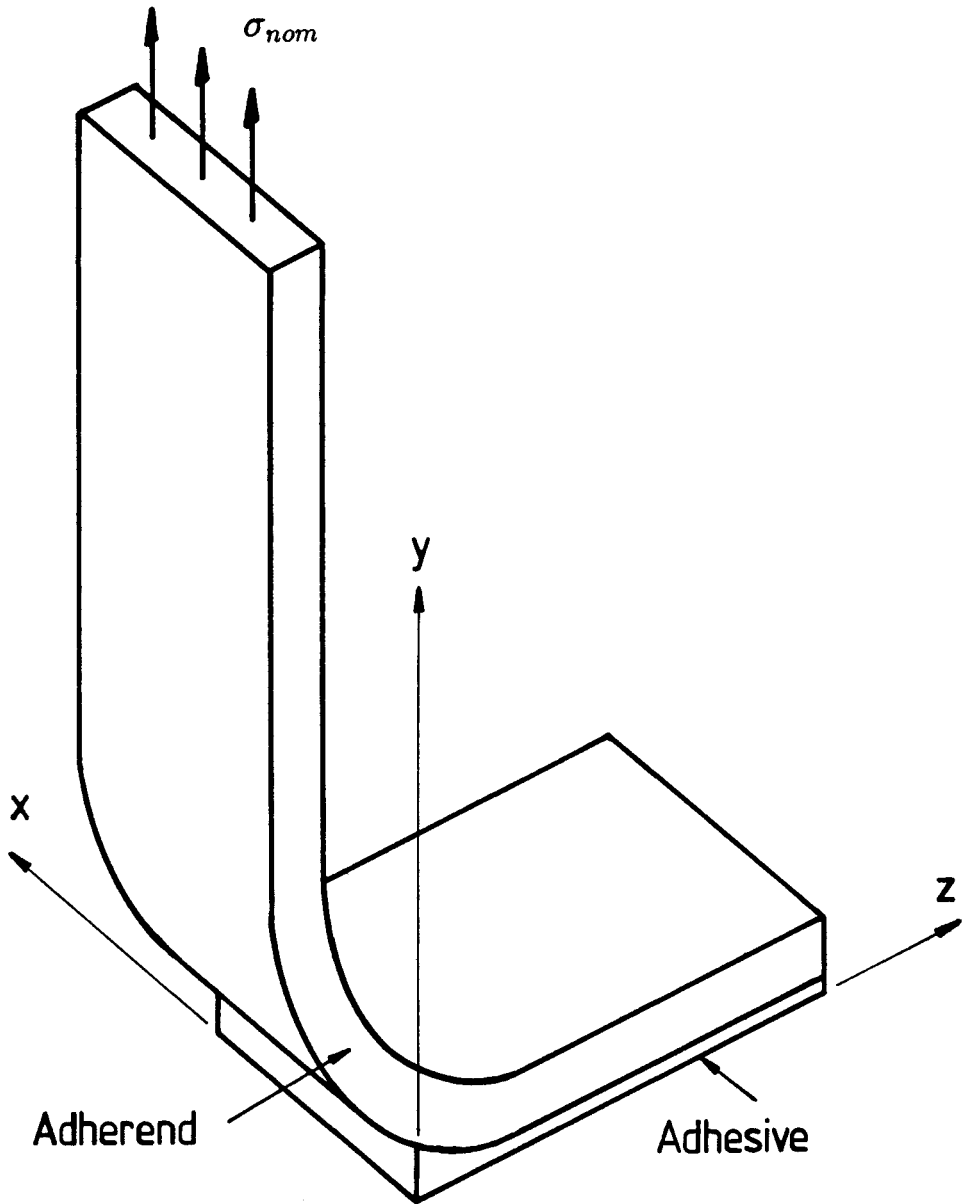
FIGURE 1 Schematic of half of a typical T-peel joint used to generate a 3D finite element mesh. The $y=0$ symmetry plane locates the centre of the bondline.

CRACK TIP STRESS CHARACTERISATION

Within cracked structures it is common to characterise the near crack-tip stress conditions in terms of either the stress intensity factor or the strain energy release rate. Whilst both K and G or the J-integral can be calculated numerically for 3D defect configurations, it is often easier to determine the variation of K than of J around the front of a 3D planar crack by using such quantities as ¼-point nodal displacements, extrapolated displacements or distributions of stress. Alternatively, the J-integral variation along a 3D crack front can be obtained by defining a suitable series of integral paths around the front. When analysing defects within composite and bimaterial structures, the J-integral can often prove more reliable than K at characterising crack-tip stress conditions. It can be difficult to use K when characterising crack stress fields adjacent to such material discontinuities as typically occur across adherend-adhesive, matrix-fibre and lamina interfaces. This is particularly true when a defect either intersects an interface or exists along an interface but is not necessarily true when it is wholly contained within one material and is remote from the interface. This difficulty is not associated with the J-integral since the strain energy release rate is independent of the particular integral path chosen, provided of course that a sufficiently fine finite element mesh is used. Consequently, an integral path intersecting a bimaterial interface will predict a value of J for a cohesive defect similar to a path which is wholly contained within that material surrounding the defect. Wang et al.[2] and Ouezdou & Chudnovsky[3] have previously shown that stress intensity factors can be used to characterise cohesive defects provided that it is the physical properties of that material surrounding the defect which are used to determine K. Gilchrist[4] has also compared J-integral based estimates of stress intensity factor with K values calculated from the out-of-plane cracked ¼-point nodal displacements[5,6] when using 2D finite element models of cohesive defects in bonded joints. The difference between the two methods of estimating K, from either J-integrals or ¼-point nodal displacements, was less than 1%. Such close agreement indicates that for linear cohesive crack growth it is valid to characterise crack-tip stress conditions in terms of either the J-integral or the stress intensity factor.

Wassell et al.[7] have investigated the cohesive fatigue crack propagation within a common rubber-toughened epoxy adhesive used to bond adherends of aluminium alloy 6082 TF. The material properties of both adhesive and adherend are given in Table I; cohesive crack propagation rates within these particular materials were found to obey a Paris type relationship

$$\frac{\mathrm{d}a}{\mathrm{d}N} = 10^{-16} \, (\Delta J_{\mathrm{I}})^{5.7}$$

where J_I has units of Joules/m^2 and crack growth rate is measured in mm/cycle. In accordance with the principles of linear elastic fracture mechanics, J is equal to the elastic strain energy, G, and is consequently related to the stress intensity factor, K. The crack growth rate can alternatively be defined by the stress intensity factor which can be obtained from the out-of-plane displacements of ¼-point cracked nodes in a manner which has been described elsewhere by the authors.[8-10] Within

TABLE I
Physical properties of aluminium adherend and epoxy adhesive

Material	E [GPa]	ν	σ_{UTS} [MPa]	σ_y [MPa]
Aluminium	70.0	0.33	220.0	95.0
Epoxy	3.2	0.35	70.0	

the analyses of this article the authors have used both K and J to characterise the defects in 2D finite element models but have only used K (appropriately converted to J-integral values to predict cohesive fatigue crack growth using the growth rate law of Wassell et al.[7]) in the series of 3D models.

COHESIVE DEFECTS IN T-PEEL JOINTS

The extent of the adhesive bond within a T-section joint can range in length over the complete fillet region. A short adhesive length provides a particularly weak bond because of the excessively offset load path. An overly long adhesive bond, however, provides the strongest possible joint but is often difficult to obtain in manufacturing situations: it is undesirable to have adhesive "slumping" from a joint prior to or during curing.[11] The distribution of tensile stress along the middle of the bond centreline for a typical adhesive length is detailed in Figure 2. The maximum stress occurs slightly inside the adhesive fillet front edge. This is followed by a region of compressive stress which decreases to zero throughout most of the bondline away from the fillet region along the flange length. The amount of adhesive in the fillet region significantly alters the bondline stresses but does not affect the characteristic distribution of stress: the magnitude of stress changes whilst the actual manner of variation is essentially the same. The adhesive directly within the load path (i.e., within the fillet region) is subject to tensile stresses with the maximum centreline stress being some distance within from the exterior surface of the adhesive. Clearly joint stresses are minimised by using as much adhesive in the fillet region of a T-section joint as possible since this is the critical load-bearing area of the joint.

Merely by changing the material properties of appropriate elements within the adhesive layer to those of adherend material provides a finite element model of a weld-bonded joint. A spot-weld can only be properly analysed with a 3D model: a 2D analysis actually models a strip-weld or a seam-weld. However, since the plane strain centreline conditions within a spot weld-bonded joint is somewhere between those of a seam weld-bonded joint and a bonded joint, a 2D analysis can be useful for predicting the likely response and performance of a spot weld-bonded joint. The tensile stress distribution along the centreline of a weld-bonded joint is detailed in Figure 3 and compared with that of a bonded joint. The most significant feature is that the maximum tensile stress of the weld-bonded joint is equal to that of the bonded joint in both magnitude and location. Since fatigue defects tend to initiate from the region of maximum tensile stress, initial cohesive crack growth in a weld-bonded joint is likely to be similar to that in a bonded joint. Initial rates of propaga-
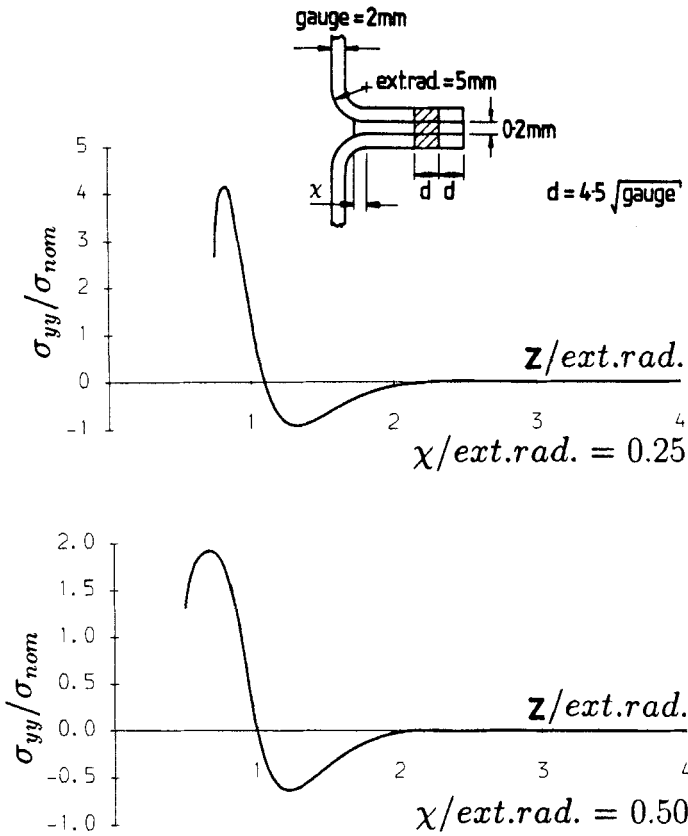
FIGURE 2 Variation of bond centreline tensile stress σ_{yy} with adhesive fillet length, $\chi/ext.\ rad.$

tion and directions of growth are also likely to be similar. The peak compressive stresses within weld-bonded joints, however, occur at the edge of the weld nugget. The physical significance of this compressive stress concentration is that defects are unlikely to initiate within this region. It is important to note that the 2D and 3D finite element models of the spot-weld are approximations to the precise physical conditions which are associated with an actual spot-weld. The complete spot-weld region has been modelled using the same material properties as the parent aluminium adherend. Similarly, the small adhesive-free annulus which surrounds the spot-weld has been ignored. These assumptions, although somewhat crude, enable the finite element models to provide indicative results of the conditions which exist around a spot-weld in relation to the adhesive bondline.

A typical 2D T-peel finite element model is shown in Figure 4 together with mesh detail in the vicinity of the adherend-adhesive interface. Model symmetry along the bond centreline is defined by restraining the vertical (y-axis) displacements of uncracked nodes on the y=0 plane. Rigid body motions are prevented by fully
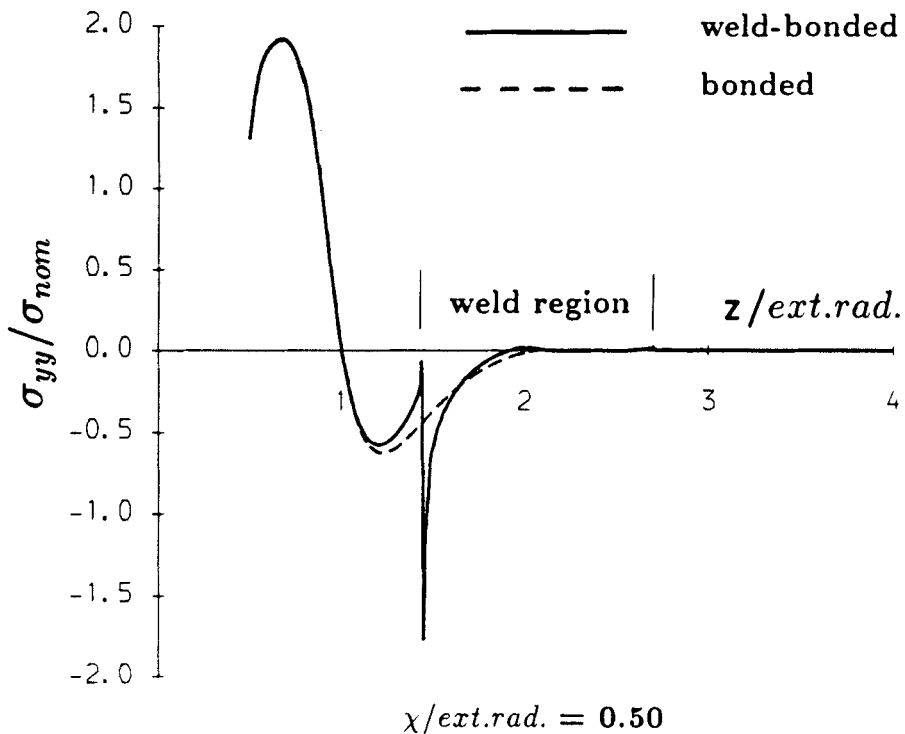
$$\chi/ext.rad. = 0.50$$

FIGURE 3   Distribution of centreline stress σ_{yy} within bonded and weld-bonded T-peel joints.

restraining that node on the $y = 0$ plane which is furthest removed from the joint edge. The elements are all 2D isoparametric quadrilaterals with midside and vertex nodes and 3×3 integration points. Six elements through the 0.1 mm adhesive layer half-thickness consequently represent the model variables at eighteen Gaussian integration points from the bond centreline to the adherend-adhesive interface. The adhesive elements are analysed as plane strain to simulate interior conditions within a 3D T-peel joint. The mesh layout within the adhesive is significantly finer than within the adherend. This is necessary to estimate accurately the distribution of stress throughout the adhesive layer, especially adjacent to the fillet where the tensile stresses and gradients of stress are greatest. Modelling the adhesive half-thickness with six elements was sufficient to calculate the critical stresses. Coarser models used by the authors[4] (not detailed here), which had only six integration points through the adhesive half-thickness, did not provide the same degree of accuracy as the finer meshes; the results of such meshes are not discussed further within this article.

Due to the composition of the epoxy adhesive with its random distribution of defects such as voids, calcium silicate filler particles and rubber-toughening particles, all of which can act as stress concentrations, it is postulated that crack growth tends to initiate at that defect(s) which is within (or closest to) the region of
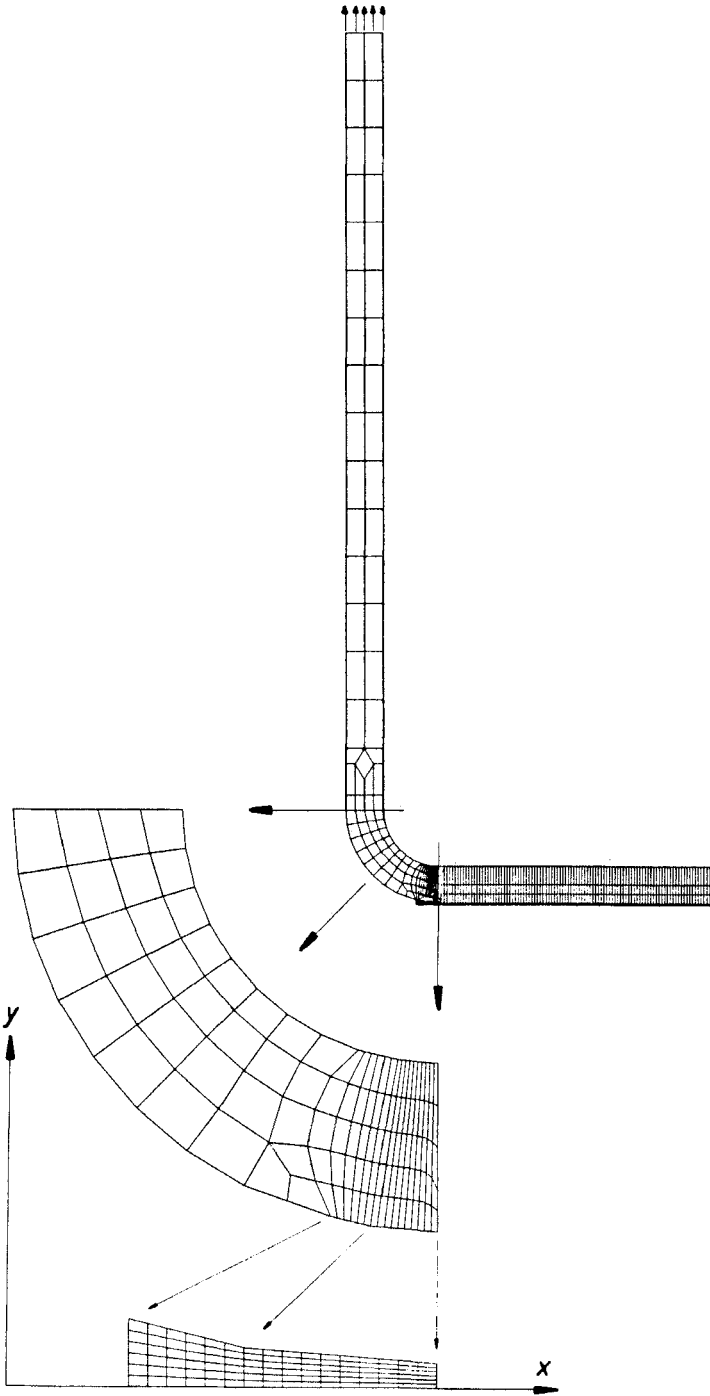
FIGURE 4   Typical 2D finite element mesh of half T-peel joint showing enlarged detail of fillet region.

maximum tensile stress. By appropriate expansions of a 2D finite element model, utilising planes of symmetry wherever possible to minimise computational requirements and by releasing appropriate nodes along the adhesive centreline, a 3D model of a planar, initially-circular defect within the fillet region of a T-peel joint was created. A coarse planar mesh of the adhesive midplane is shown in Figure 5. This corresponds to the $y = 0$ plane of Figure 1. The relative proximity of the postulated defect to the adhesive fillet front edge is quite apparent. Further specific details of these finite element models are provided by Gilchrist.[4]

A typical variation of strain energy release rate around such an embedded defect is shown in Figure 6 in order to indicate the likely direction in which this defect will propagate. The J-integral at the crack front point closest to the adhesive fillet front surface (C) is maximum. That point furthest from the surface (A) also has a relatively high growth rate whilst the lateral crack front point (B) has minimum values
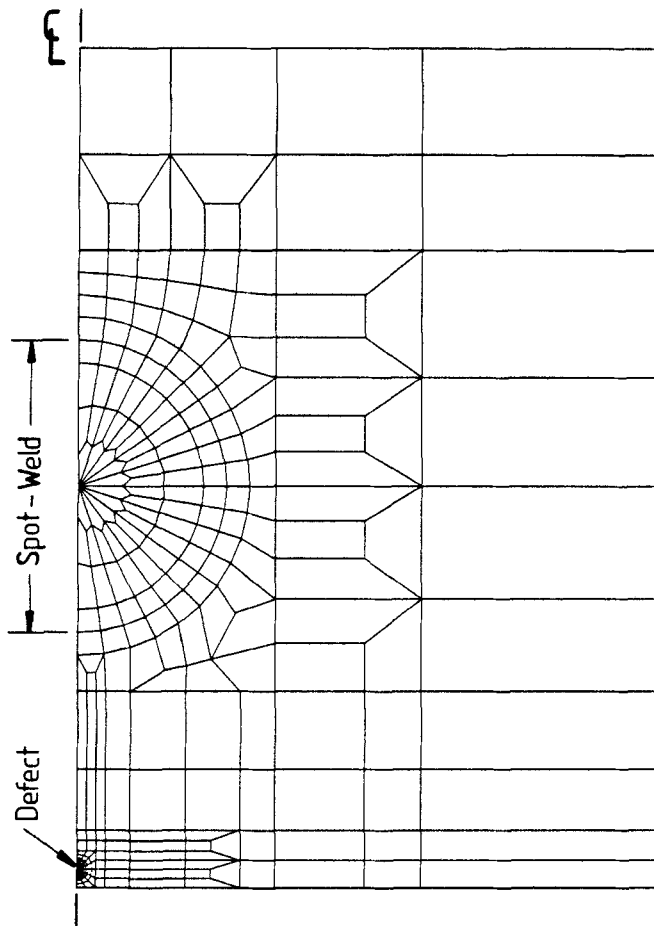
FIGURE 5 Section of 3D finite element mesh showing postulated defect and spot-weld. This corresponds to $y = 0$ plane of Figure 1.
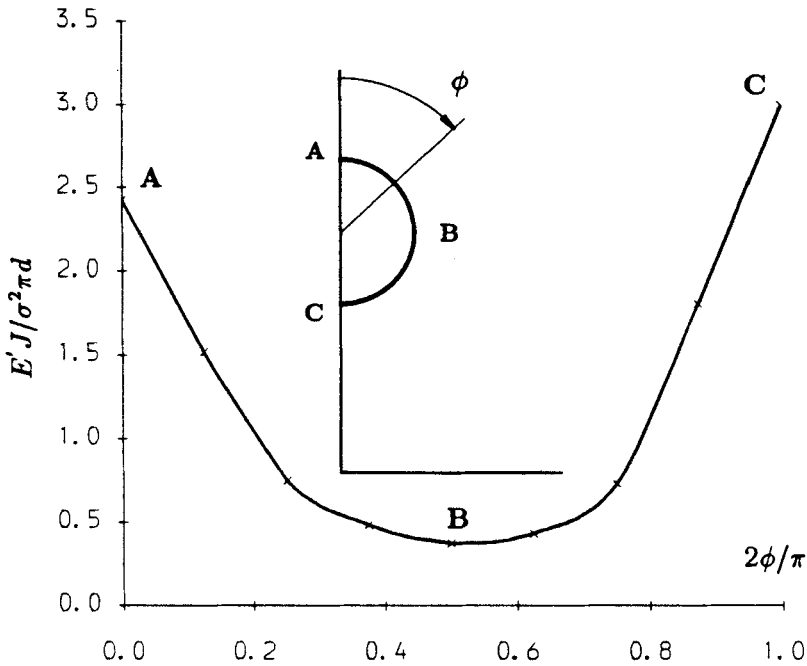
FIGURE 6 Variation of normalised strain energy release rate around postulated embedded defect which lies in the adhesive fillet region of joint.

of J. Since cohesive crack growth is related to a power of J this initially circular defect (postulated to initiate in the region of maximum tensile stress) tends to adopt an elliptical profile with major and minor axes being normal and parallel to the exterior surfaces of the adhesive fillet edge. The degree of ellipticity and number of fatigue cycles to defect breakout can be calculated by assuming a number of fatigue cycles within Wassell's growth law, advancing the initial defect by the consequent increments of crack growth, creating and analysing a new 3D model of the cohesive defect and T-peel joint and repeating this process iteratively. However, such intensive numerical calculations can be avoided by characterising the defect growth into three different stages and estimating the relative fatigue life of each stage by using appropriate empirical formulae. The stages of growth are detailed with their respective fatigue lives in Figure 7 and are as follows:

1: From an initial embedded circular defect until breakout. Crack growth is assumed to be elliptical. Stress intensity factors are calculated at the points A and B on the crack front using Newman & Raju's equations[12] for embedded elliptical cracks. Increments of crack growth are calculated from the growth law of Wassell et al.[7] An ellipse is subsequently fitted to the new defect which is allowed to propagate to breakout on a cycle-by-cycle basis.

2: At breakout the defect is recharacterised as a semi-elliptical surface defect. K is estimated at the surface and depth points of the defect using Newman &
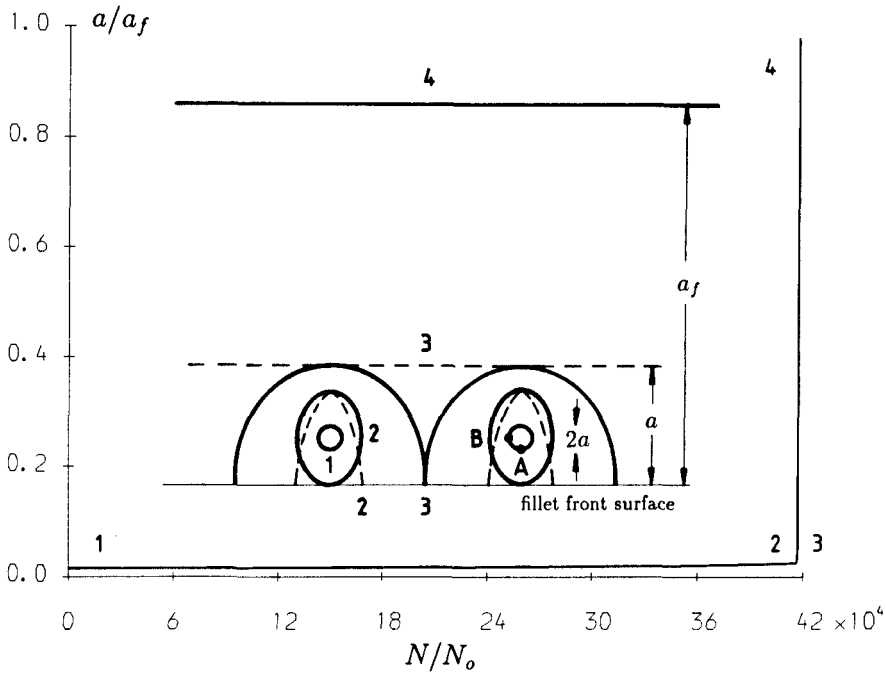
FIGURE 7 Approximate estimates of the relative fatigue life of different stages of cohesive defect growth. The only significant life is from an embedded profile until breakout at the adhesive fillet front edge. The same uniform tension was assumed for each stage of growth.

Raju's equations[12] for semi-elliptical surface defects. Crack growth calculated as for stage 1 is modelled in this way until a defect reaches the lateral external surfaces of the T-peel joint. If defects coalesce during this stage as typically shown in Figure 7 (this depends on the assumed pitch of the initial defects) they are replaced by a single bounding semi-elliptical defect.

3: The third stage of the characterisation approximates the lateral breaking defect(s) as a single straight-through, through-width defect, K being calculated by Brown & Srawley's 2D equation[13] and crack growth being modelled through the remaining adhesive section.

The dimensionless fatigue cycles of Figure 7 are related to the specimen dimensions, material growth rate properties and loading conditions:

$$N_0 = \frac{w}{C(\Delta\sigma\sqrt{\pi w})^m}$$

This manner of normalising fatigue crack growth enables the results of different analyses to be directly compared for different specimen dimensions, material growth rate coefficients and loading conditions. It is clear from Figure 7 that the only significant stage of fatigue crack growth is the initial stage, i.e., from an embedded defect until breakout at the adhesive fillet front edge. Approximately 95% of fatigue

life is consumed within this stage. Fatigue life was considered to be the number of cycles required to propagate the defect from its initial embedded location to final fracture. The same tensile fatigue load was assumed for each stage of growth; this is reasonable for an approximate estimate of fatigue life. The fatigue cycles detailed in Figure 7 are normalised and are not absolute fatigue cycles. It is clearly evident that a T-peel joint fails almost immediately after an initially-embedded defect breaks out at the adhesive fillet front edge to form a single through-width defect.

CONCLUSIONS

The fatigue growth of planar defects within adhesively-bonded T-peel joints has been modelled. Crack growth was assumed to be cohesive rather than adhesive with defects remaining within the adhesive layer away from adherend surfaces. In accordance with linear elastic fracture mechanics, crack growth was characterised using both stress intensity factors and strain energy release rates. The initiation and fatigue growth of defects within adhesively-bonded and weld-bonded T-peel joints has been investigated. It has been found that defects are most likely to initiate cohesively within the adhesive fillet region, propagate to the surface, form a through-width defect and rapidly grow through the remaining bond. Joint failure occurs shortly after breakout from the initially-embedded location. Joint static and fatigue strengths are maximised by having a maximum amount of adhesive within the fillet region.

Acknowledgments

References

1. A. R. Woodward, *Aluminium Industry* **9** (5), 31–34 (1990).
2. S. S. Wang, J. F. Mandell and J. F. McGarry, *Int. J. Fract.* **14** (1) 39–58 (1978).
3. M. Ben Ouezdou and A. Chudnovsky, *Engng Fract. Mechs.* **29** (3), 253–261 (1988).
4. M. D. Gilchrist, "Crack shape development in plates and bonded joints." PhD thesis, University of Sheffield (Sept. 1991) U.K.
5. R. D. Henshell and K. G. Shaw, *Int. J. Numer. Methods in Engng* **9**, 495–507 (1975).
6. R. S. Barsoum, *Int. J. Numer. Methods in Engng* **10**, 25–37 (1976).
7. G. C. Wassell, J. D. Clark, J. S. Crompton and R. F. Dickson, *Int. J. Adhesion and Adhesives* **11** (2), 117–120 (1991).
8. M. I. Chipalo, M. D. Gilchrist and R. A. Smith, *Int. J. Mech. Sci.* **32** (3), 243–251 (1990).
9. M. D. Gilchrist and R. A. Smith, *Fatigue Fract. Engng Mater. Struct.* **14** (6), 617–626 (1991).
10. M. D. Gilchrist M. I. Chipalo and R. A. Smith, *Int. J. Pres. Ves. & Piping* **49**, 121–137 (1992).
11. P. G. Sheasby and M. J. Wheeler, "Aluminium structured vehicle technology: a review." Proc. 3rd international symposium on Aluminium and automobile (3–4 Feb. 1988), Dusseldorf.
12. J. C. Newman, Jr. and I. S. Raju, *Engng Fract. Mechs.* **15** (1–2), 185–192 (1981).
13. W. F. Brown, Jr. and J. E. Srawley, **ASTM STP 410** (ASTM, Philadelphia, 1966).